

# Causal Inference for Heritable Phenotypic Risk Factors Using Heterogeneous Genetic Instruments

Jingshu Wang<sup>1,\*</sup>, Qingyuan Zhao<sup>2</sup>, Jack Bowden<sup>3</sup>, Gibran Hemani<sup>4</sup>, George Davey Smith<sup>4</sup>, Dylan S. Small<sup>5</sup>, Nancy R. Zhang<sup>5</sup>, and <sup>2</sup>

<sup>1</sup>*The University of Chicago*

<sup>2</sup>*University of Cambridge*

<sup>3</sup>*The University of Exeter*

<sup>4</sup>*University of Bristol*

<sup>5</sup>*University of Pennsylvania*

\* [jingshuw@uchicago.edu](mailto:jingshuw@uchicago.edu)

## Abstract

Over a decade of genome-wide association studies have led to the finding that significant genetic associations tend to spread across the genome for complex traits. The extreme polygenicity where “all genes affect every complex trait” complicates Mendelian Randomization studies, where natural genetic variations are used as instruments to infer the causal effect of heritable risk factors. We reexamine the assumptions of existing Mendelian Randomization methods and show how they need to be clarified to allow for pervasive horizontal pleiotropy and heterogeneous effect sizes. We propose a comprehensive framework GRAPPLE (Genome-wide mR Analysis under Pervasive PLEiotropy) to analyze the causal effect of target risk factors with heterogeneous genetic instruments and identify possible pleiotropic patterns from data. By using summary statistics from genome-wide association studies, GRAPPLE can efficiently use both strong and weak genetic instruments, detect the existence of multiple pleiotropic pathways, adjust for confounding risk factors, and determine the causal direction. With GRAPPLE, we analyze the effect of blood lipids, body mass index, and systolic blood pressure on 25 disease outcomes, gaining new information on their causal relationships and the potential pleiotropic pathways.

# 1 Introduction

Understanding the pathogenic mechanism of common diseases is a fundamental goal in clinical research. As randomized controlled experiments are not always possible, researchers are looking towards Mendelian Randomization (MR) as an alternative method for probing the causal mechanisms of common diseases [18]. MR uses inherited genetic variations as instrumental variables (IV) to interrogate the causal effect of heritable risk factor(s) on the disease of interest. The basic idea is that at these variant loci, the inherited alleles are randomly transmitted from the parents to their offsprings according to Mendel’s laws. Thus, the genotypes are independent from non-heritable confounding variables which may obfuscate causal estimation in parent-offspring studies. More generally, such independence also approximately holds for population data such as the genome-wide association studies (GWAS) when individuals share the same ancestry [46]. With the accumulation of data from GWAS, there is an increasing interest in MR approaches, especially approaches that only rely on the GWAS summary statistics that are readily available in the public domain [19, 46].

How well Mendelian Randomization works depends on how well the genetic variant loci used as instruments abide by the rules of IV. These rules dictate that, if the genetic locus has an effect on the disease outcome, it should be only through pathways mediated by the risk factor(s) of interest. This rule, termed exclusion restriction, is violated when there is horizontal pleiotropy, defined as the case where the genetic variant can influence the disease through pathways other than the given risk factor(s) [21]. There has been much recent attention on this issue [10, 4, 5, 25, 51, 59, 42, 11, 3, 36, 43] in MR, yet our understanding is far from complete. Current methods rely on different assumptions on the pattern of horizontal pleiotropy, while improper assumptions may lead to biased estimation of the true causal effects. What assumptions on pleiotropy and genetic effects would be suitable? Would it be possible to learn the degree of pleiotropy from the data? Could we perform model diagnosis utilizing only GWAS summary statistics?

The pleiotropy issue that muddles Mendelian Randomization studies is, in a large part, due to the fact that complex traits are extremely polygenic [16, 57, 8, 32, 45, 49, 36, 38, 55]. Accumulating evidence from GWAS studies indicate that complex diseases may share an omnigenic architecture where all genes affect every complex trait [6]. While a few genes might be “core” genes, almost all genes are involved and can exert non-zero effects on both the risk factors and disease. Thus, given a risk factor that explains only part of the causal mechanism of a complex disease, there would be many SNPs affecting the disease through their effects on other unmeasured risk factors. In other words, in an MR analysis, not only would we expect horizontal pleiotropy to be a pervasive issue across all genetic variants, any disease or complex risk factor would also be associated with a large number of SNPs across the whole genome. Many existing MR methods rely on the assumption that pleiotropic effects sparsely involve only a few SNPs, which directly counters these recent insights. Methods that don’t assume sparsity often require that the pleiotropic effects cancel each other across SNPs, named as the instrument strength independent of direct effect (inSIDE) assumption [4], which can be rather optimistic. Recently, a few new methods relaxed the inSIDE assumption to consider “directional pleiotropy” through one pleiotropic pathway [36]. However, there would then be an issue

65 in identifying the true causal effect of the risk factor, and the model is restrictive to allow for only one  
66 pleiotropy pathway. Armed with these assumptions, most existing methods also utilize only the few  
67 SNPs that have the strongest association with the risk factor as instruments, ignoring the SNPs that  
68 are weakly associated. In this work, we will show that weakly associated SNPs are also informative,  
69 and that a model combining weak and strong SNPs would not harm MR while increasing its accuracy  
70 and stability in some scenarios.

71 We propose a comprehensive statistical framework for causal effect estimation when pleiotropy is  
72 pervasive across the genome. The framework, called GRAPPLE (Genome-wide mR Analysis under  
73 Pervasive PLEiotropy), facilitates interactive identification of multiple pleiotropic pathways and the  
74 incorporation of all SNPs associated with the risk factor into the analysis. GRAPPLE builds on the  
75 statistical framework MR-RAPS [59]. However, we emphasize the detection of multiple pleiotropic  
76 pathways when the inSIDE assumption in MR-RAPS is violated as well as the discrimination of  
77 the direction of causality. Using GRAPPLE, we further address how to jointly estimate the effects  
78 with multiple risk factors to reduce directional pleiotropy, as well as how to integrate cohorts with  
79 overlapping samples, both common challenges faced by current studies. The estimation accuracy of  
80 GRAPPLE is examined through validations involving real studies and simulations.

81 GRAPPLE is applied to a screening of the causal effects of 5 risk factors (three plasma lipid  
82 traits, body mass index, and systolic blood pressure) on 25 common diseases. Although there have  
83 been many causal effect screens [51, 39, 36] for these risk factors and diseases, the combined analysis  
84 enabled by GRAPPLE brings forth new insights on the pleiotropic landscape across diseases and,  
85 thus, an improved understanding of the causal estimates obtained. Specifically, we will reexamine  
86 the role of lipid traits on coronary artery disease and type-II diabetes, where the results from the  
87 multitude of MR studies [46, 31, 33] have been under heated debate.

## 88 2 Results

### 89 2.1 Model Overview

#### 90 2.1.1 From the causal model to GWAS summary statistics

91 Our framework starts with a set of structural equations that jointly specify the generative model on  
92 the disease  $Y$  that relies on  $K$  observed risk factors  $\mathbf{X} = (X_1, \dots, X_K)$  of interest, and all genetic  
93 variants  $\mathbf{Z} = (Z_1, Z_2, \dots)$  (Fig 1a).

$$\begin{aligned} Y &= \mathbf{X}^T \boldsymbol{\beta} + f(\mathbf{U}, \mathbf{Z}, E_Y) \quad (\text{if } Y \text{ is a continuous trait}) \\ \text{logit}[P(Y = 1)] &= \mathbf{X}^T \boldsymbol{\beta} + f(\mathbf{U}, \mathbf{Z}, E_Y) \quad (\text{if } Y \text{ is a binary trait}) \\ X_k &= g_k(\mathbf{U}, \mathbf{Z}, E_{X_k}), \quad k = 1, \dots, K \end{aligned} \tag{1}$$

94 where  $\mathbf{U}$  represents unknown non-heritable confounding factors and  $E_{X_k}$  and  $E_Y$  are random noise  
95 acting on  $X_k$  and  $Y$  respectively. The parameter of interest,  $\boldsymbol{\beta}$ , quantifies the causal effect of the

96 vector of risk factors  $\mathbf{X}$  on  $Y$ . Due to Mendel's law of inheritance, the genotypes  $\mathbf{Z}$  are independent  
97 of  $(\mathbf{U}, E_Y, E_{X_k})$ . The function  $f(\mathbf{U}, \mathbf{Z}, E_Y)$  represents the causal effect of unmeasured risk factors  
98 on  $Y$ , which can be heritable (contributed by  $\mathbf{Z}$ ) or non-heritable (contributed by  $\mathbf{U}$ ). The non-  
99 parametric functions  $f(\cdot)$  and  $g_k(\cdot)$  allow interactions among SNPs in  $\mathbf{Z}$  and variables  $(\mathbf{U}, E_Y, E_{X_k})$   
100 in their causal effects on  $\mathbf{X}$  and  $Y$ . Under this model, there is horizontal pleiotropy for a SNP  $j$  if  $Z_j$   
101 has nonzero association with  $f(\mathbf{U}, \mathbf{Z}, E_Y)$ . This is the case, for example, when  $Z_j$  acts on  $Y$  through  
102 a pathway affecting unmeasured risk factors, or when  $Z_j$  is in linkage disequilibrium (LD) with such  
103 a locus.

104 Now consider the case where only GWAS summary statistics, i.e. the estimated marginal asso-  
105 ciations between each SNP  $j$  and the risk factors/disease traits, are available. Let  $\Gamma_j$  be the true  
106 association between SNP  $j$  and  $Y$ , and  $\boldsymbol{\gamma}_j$  be the vector of true marginal associations between SNP  
107  $j$  and  $\mathbf{X}$ . Later, we will denote their estimated values from GWAS summary statistics as  $\hat{\Gamma}_j, \hat{\boldsymbol{\gamma}}_j$ .  
108 Then, as shown in Materials and Methods, the model (1) results in the linear relationship

$$\Gamma_j = \boldsymbol{\gamma}_j^T \boldsymbol{\beta} + \alpha_j \quad (2)$$

109 where for binary  $Y$ , the parameter  $\boldsymbol{\beta}$  in (2) is a conservatively biased version of  $\boldsymbol{\beta}$  in (1). This  
110 relationship holds even when the functions  $f(\cdot)$  and  $g(\cdot)$  in (1) are not linear. Here,  $\alpha_j$  is the marginal  
111 association between  $Z_j$  and  $f(\mathbf{U}, \mathbf{Z}, E_Y)$ , representing the unknown horizontal pleiotropy of SNP  $j$ .  
112 In MR, one would typically simultaneously select  $p$  SNPs as multiple instruments to estimate the  
113 causal effect of  $\mathbf{X}$ .

114 One can immediately see that identifying  $\boldsymbol{\beta}$  is impossible without further assumptions on  $\alpha_j$ .  
115 Early MR methods such as IVW [10] made the simplest assumption that all instruments are valid  
116 satisfying  $\alpha_j = 0$ . However, as already discussed in Introduction, the assumption of no pleiotropy, or  
117 more generally, assuming that  $\alpha_j$  is sparsely nonzero as in Weighted Median [5] or MR-PRSSO [51]  
118 contradicts the fact that horizontal pleiotropy is pervasive. One assumption that allows pervasive  
119 pleiotropy is to assume the inSIDE assumption [4] where  $\alpha_j \perp \boldsymbol{\gamma}_j$ , or alternatively, the random  
120 effect model [59, 43] where  $\alpha_j \sim \mathcal{N}(0, \tau^2)$  for most genetic instruments. Unfortunately, the inSIDE  
121 assumption requires all unmeasured heritable risk factors of the disease to be genetically uncorrelated  
122 with the target risk factor(s)  $\mathbf{X}$ , which is likely violated, especially when there are clusters of SNPs  
123 associate with both the unmeasured risk factors and  $\mathbf{X}$ .

124 Noticing the limitation of the inSIDE assumption, some new MR methods, such as LCV [39],  
125 CAUSE [36] and MRMix [42] allow a proportion of genetic instruments to be associated with one  
126 common hidden pleiotropic pathway affecting both the risk factor and disease. For instance, under  
127 the above notation, both CAUSE and MRMix assumed that for the proportion of SNPs that violate  
128 the inSIDE assumption, their pleiotropic effects satisfy  $\alpha_j = \boldsymbol{\gamma}_j^T \mathbf{a} + \tilde{\alpha}_j$  where  $\boldsymbol{\gamma}_j^T \mathbf{a}$  represents the  
129 directional pleiotropic effects due to a confounding pathway and  $\tilde{\alpha}_j \perp \boldsymbol{\gamma}_j$ . This is a more realistic  
130 assumption than inSIDE, though there would then be an issue to distinguish the true causal effect  
131  $\boldsymbol{\beta}$  from the pleiotropic direction  $\boldsymbol{\beta} + \mathbf{a}$ , and the model may be too restrictive to allow for only one  
132 pleiotropic pathway.

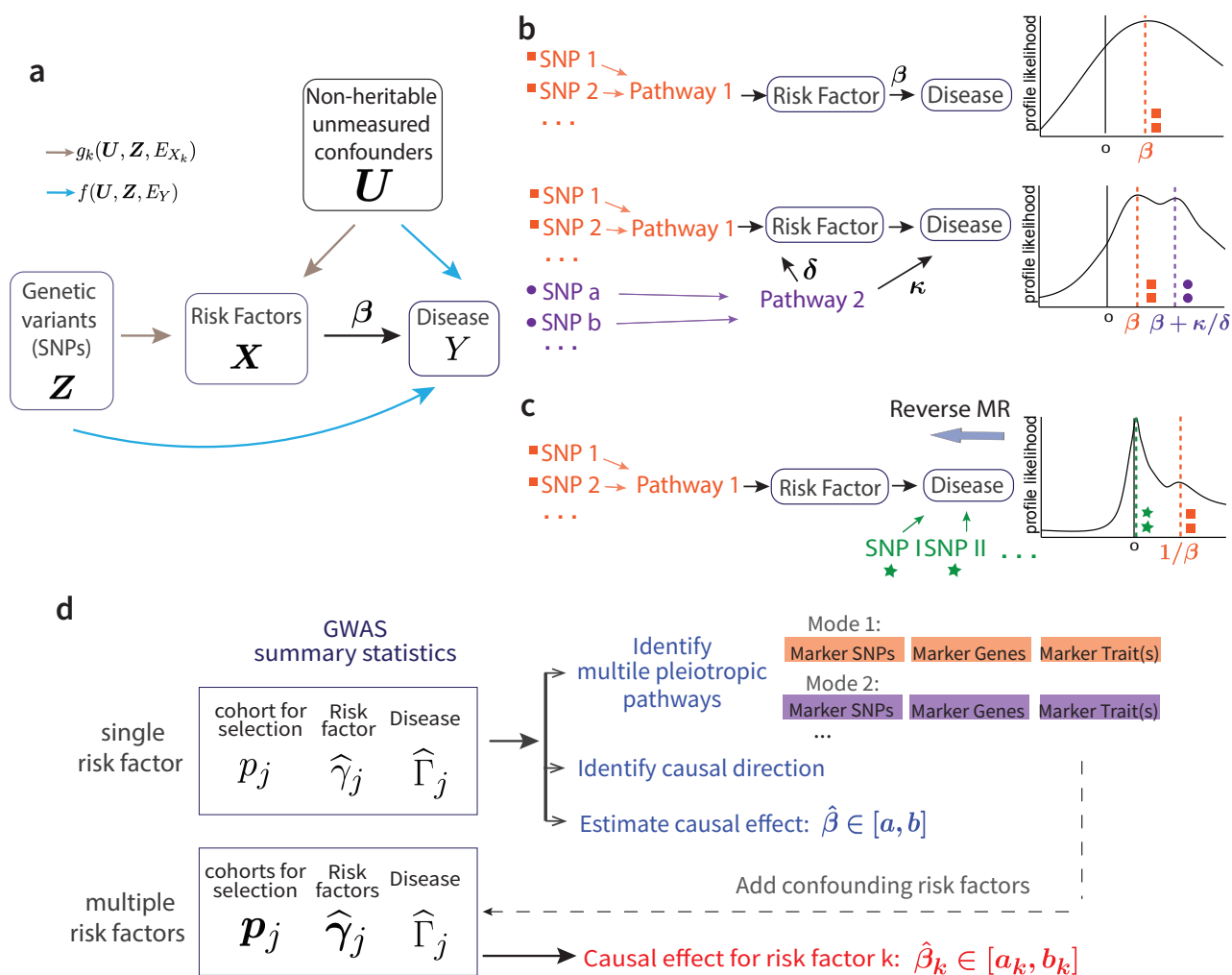


Figure 1: Model overview. **a**, The causal directed graph represented by structural equations (1). **b**, The existence of a pleiotropic pathway 2 (purple) can result in multiple modes of the profile likelihood. **c**, Multi-modality of the profile likelihood can reflect causal direction. **d**, The work-flow with GRAPPLE.

### 2.1.2 Identify multiple pleiotropic pathways and the direction of causality

The key idea underlying GRAPPLE is to detect multiple pleiotropic pathways by using the shape of the data profile likelihood under no pleiotropy to probe the underlying causal mechanism, without explicit assumptions of the pleiotropic patterns (Fig 1b). When  $K = 1$ , the GWAS summary statistics reduce to the scalar  $\hat{\gamma}_j$  and  $\hat{\Gamma}_j$ , with their standard errors  $\sigma_{1j}^2$  and  $\sigma_{2j}^2$ . From the central limit theorem, the joint distribution of  $(\hat{\gamma}_j, \hat{\Gamma}_j)$  approximately follows a multivariate normal distribution

$$\begin{pmatrix} \hat{\gamma}_j \\ \hat{\Gamma}_j \end{pmatrix} \sim \mathcal{N} \left( \begin{pmatrix} \gamma_j \\ \Gamma_j \end{pmatrix}, \begin{pmatrix} \sigma_{1j}^2 & \sigma_{1j}\sigma_{2j}\theta \\ \sigma_{1j}\sigma_{2j}\theta & \sigma_{2j}^2 \end{pmatrix} \right) \quad (3)$$

where  $\theta$  is a shared sample correlation that can be estimated as  $\hat{\theta}$  (see Materials and Methods).

When there is no horizontal pleiotropy in the  $p$  selected independent genetic instruments ( $\alpha_j = 0$

for  $j = 1, 2, \dots, p$ ), the robustified profile likelihood is [59],

$$l(b) = - \sum_{j=1}^p \rho \left( \frac{\hat{\Gamma}_j - b\hat{\gamma}_j}{\sqrt{\sigma_{1j}^2 + b^2\sigma_{2j}^2 + 2b\hat{\theta}\sigma_{1j}\sigma_{2j}}} \right) \quad (4)$$

where  $\rho(\cdot)$  is the Tukey's Biweight loss. As described with more details in Materials and Methods, the profile likelihood is obtained by profiling out nuisance parameters  $\gamma_1, \dots, \gamma_p$  in the full likelihood from (3), which is further robustified by replacing the  $L_2$  loss with Tukey's Biweight loss to increase the sensitivity of mode detection. Under no pleiotropy or inSIDE assumption, it would only have one mode near the true causal effect  $b = \beta$ .

Now consider the case where a second genetic pathway (Pathway 2) also contributes substantially to the disease, and where some of the loci that we include as instruments are also associated with Pathway 2 (Fig 1b). In this scenario, SNPs that are associated with  $X$  only through Pathway 2 can contribute to a second mode in the profile likelihood at location  $\beta + \kappa/\delta$ , where  $\kappa$  and  $\delta$  quantifies the causal effect of Pathway 2 on  $Y$  and its marginal association with  $X$ , respectively (Materials and Methods). By a similar logic, multiple pleiotropic pathways result in multiple modes in  $l(b)$ . Thus, we can use the presence of multiple modes in  $l(b)$  to diagnose the presence of horizontal pleiotropic effects that are grouped into different directions.

The existence of pleiotropic pathways not only complicates MR, more severely, it makes the causal effects of the risk factors unidentifiable. Specifically, when Pathway 2 exists, the GWAS summary statistics alone can not provide information to distinguish  $\beta$  from  $\beta + \kappa/\delta$ . Instead of making further assumptions to identify the true causal effect, when multiple modes are detected, we suggest collecting more GWAS data to adjust for confounding risk factors that contribute to these modes. To help finding the confounding risk factors, GRAPPLE identifies marker SNPs of each mode, as well as the mapped genes and GWAS traits of each marker SNP (see Materials and Methods), so that researchers can use their expert knowledge to infer possible confounding risk factors that contribute to each mode. With the GWAS summary statistics of these confounding traits, GRAPPLE can perform a multivariate MR analysis assuming the inSIDE assumption on the remaining horizontal pleiotropic effects. GRAPPLE uses an adjusted robustified profile likelihood approach that can jointly estimate  $\beta$  and  $\tau^2$  (Materials and Methods).

With multiple modes detection, we can also consider the question of whether  $X$  indeed causes  $Y$ , as our structural equation (1) presumes, or it is the reverse case of  $Y$  causing  $X$ . If it were the case that the direction of causality runs from  $Y$  to  $X$ , then an instrument is associated with  $X$  either through  $Y$ , or through unmeasured heritable risk factors of  $X$  unrelated to  $Y$ . In the latter case, a SNP  $j$  satisfies  $\gamma_j \neq 0$  while  $\Gamma_j = 0$ , and would contribute to a mode at 0. In the former case,  $\gamma_j = \beta\Gamma_j$  where  $\beta$  is the causal effect of  $Y$  on  $X$ , and these SNPs may contribute to a mode around  $1/\beta$ . This idea shares similarities with bidirectional MR [50, 26]. Bidirectional MR is based on the assumptions that when MR is reversely performed, all selected instruments affect  $Y$  not through  $X$ , and filters out suspicious SNPs that may violate this assumption by checking their associations with



176  $X$ . Though it sometimes works, there is no guarantee that the filtering does not introduce bias. In  
177 GRAPPLE, we identify the direction by checking if there is a mode at 0 after switching the roles of  
178  $X$  and  $Y$ , while tolerating the existence of another mode around  $1/\hat{\beta}$ .

### 179 **2.1.3 Weak genetic instruments: A curse or a blessing?**

180 Besides the assumption of no-horizontal-pleiotropy, for a SNP to be a valid genetic instrument, it  
181 needs to have a non-zero association with the risk factor of interest. In most MR pipelines, SNPs are  
182 selected as instruments only when their p-values are below  $10^{-8}$ , which is required to guarantee a low  
183 family-wise error rate (FWER) for GWAS data. Using such a stringent threshold also avoids weak  
184 instrument bias [13], where measurement errors in  $\hat{\gamma}_{jk}$  are too large to lead to bias in  $\hat{\beta}$ . However,  
185 such a stringent selection threshold may result in very few, or even zero, instruments for under-  
186 powered GWAS, and may still not be adequate to avoid weak instrument bias. Further, when our  
187 goal is to jointly model the effects of multiple risk factors (the setting where  $\mathbf{X}$  as a vector), it is  
188 unrealistic to assume that all selected SNPs have strong effects on every risk factor. In addition, the  
189 highly polygenecity phenomenon of complex traits indicates that the number of weak instruments far  
190 outnumbers the number of strong instruments, and collectively, they may exert a positive effect on  
191 the estimation accuracy.

192 In GRAPPLE, we use a flexible p-value threshold, which can be either as stringent as  $10^{-8}$  or as  
193 mild as  $10^{-2}$ , for instrument selection. Based on the profile likelihood framework of MR-RAPS [58],  
194 GRAPPLE can provide valid inference of  $\hat{\beta}$  to avoid weak instrument bias for multiple risk factors  
195 with SNPs selected at any given p-value threshold, when horizontal pleiotropy of most SNPs follow the  
196 random effect model  $\alpha_j \sim \mathcal{N}(0, \tau^2)$ . This flexible p-value threshold is beneficial for several reasons.  
197 First, including moderate and weak instruments may increase power, especially for under-powered  
198 GWAS data where there are too few strongly associated SNPs. Second, for MR with multiple risk  
199 factors where it is inevitable to include SNPs that have weak associations with some of the risk factors,  
200 we can obtain more accurate causal effect estimations than methods that can only deal with strongly  
201 associated SNPs. More importantly, comparing estimates across a series of p-value thresholds can  
202 show stability of our estimates and a more complete picture of the underlying horizontal pleiotropy.  
203 In practice, we suggest researchers to vary the selection p-value thresholds from a stringent one (say  
204  $10^{-8}$ ) to a mild one (say  $10^{-2}$ ), both in the detection of multiple modes and in estimating causal  
205 effects. We would expect to see consistent results across the p-value thresholds, if there are truly  
206 multiple pleiotropic pathways or our assumptions hold in estimating the causal effects of the risk  
207 factors.

### 208 **2.1.4 The three-sample design to guard against instrument selection bias**

209 Selecting instruments from GWAS summary statistics can also introduce bias, which is the “winner’s  
210 curse”. The magnitude of  $\hat{\gamma}_{jk}$  will increase conditional on being selected and would bias the estimate  
211 of  $\beta$ . When  $K = 1$  that there is only one risk factor, the estimate will bias towards 0, but there is

no guarantee of the direction of the bias when  $K > 1$ . Typically, it is believed that the selection bias is negligible when only the strongly associated SNPs are selected as instruments.

However, we find that for commonly used MR methods, instrument selection can introduce bias even when only genetic variants with genome-wide significant p-values ( $\leq 10^{-8}$ ) are selected (Fig S1a). Thus, unlike the usual two-sample GWAS summary statistics design which involves one GWAS data for the risk factor and one for the disease, we strongly advocate using a three-sample GWAS summary statistics design (Fig 1d). To avoid the selection bias, selection of genetic instruments is done on another GWAS dataset for the risk factor, whose cohort has no overlapping samples with both the risk factor and disease cohorts. In addition, to ease calculation (see Materials and Methods), currently we only include independent SNPs in GRAPPLE and we use the LD clumping for SNP selection to obtain them [41]. The three-sample design will also avoid possible selection bias introduced during clumping.

Summarizing the above points, a complete diagram of the GRAPPLE workflow is shown in Fig 1d. A researcher may start with a single target risk factor of interest. The shape of the robustified profile likelihood provides information on possible pleiotropic pathways. If multiple modes are detected, then one may need to adjust for pleiotropic pathways. Unfortunately, this step can not be done automatically as summary statistics themselves do not provide enough information to distinguish a causal mode from a pleiotropic mode. Researchers can use the marker SNP/gene/trait information that GRAPPLE provides to understand each mode, decide what confounding risk factors to adjust for, and collect extra GWAS data for them. GRAPPLE can then jointly estimate the causal effects of multiple risk factors to adjust for the confounding effects of the added risk factors.

## 2.2 Assessment of GRAPPLE with real studies

### 2.2.1 Inference from both weak and strong genetic instruments under no pleiotropy

We first examine whether GRAPPLE provides reliable statistical inference combining weak and strong instruments under an artificial setting with real GWAS summary statistics. In this setting, we make  $X$  and  $Y$  be the same trait from two non-overlapping cohorts, thus  $\gamma_j = \Gamma_j$  while  $\hat{\gamma}_j \neq \hat{\Gamma}_j$  for any SNP. Though the structural equation describing the causal effect of  $X$  on  $Y$  does not exist, the linear relationship model (2) from which we estimate  $\beta$  still holds with  $\beta = 1$  and  $\alpha_j = 0$ . In other words, we are not estimating a meaningful “casual” effect, but are in a special case where the true  $\beta$  is known, which can be used to test whether MR methods provides valid inference under no pleiotropy. Specifically, we consider three traits: Body mass index (BMI), Type II diabetes (T2D) and height from the GIANT and DIAGRAM consortium where sex-specific GWAS data are available [30, 35]. The female cohort is used to get  $\hat{\gamma}_j$  and the male cohort is used to get  $\hat{\Gamma}_j$ . As a three-sample design, the UK Biobank data for corresponding traits are used for SNP selection. The true  $\beta$  is 1, when we assume that all selected instruments have no gender-specific association with the traits. For benchmarking, we compare the performance of GRAPPLE with CAUSE [36] and other three well-adopted MR methods, inverse-variance weighted (IVW) [10], MR-Egger [4] and weighted median [5]



with the same three-sample design.

We compare across different p-value thresholds for instrument selection, ranging from a stringent threshold  $10^{-8}$  to a mild threshold  $10^{-2}$  (Fig 2a). GRAPPLE keeps providing unbiased estimates of  $\beta$  showing that it does not suffer from the weak instrument bias. Surprisingly, biases exist in other MR methods even with a stringent p-value threshold, which is most likely due to the power discrepancy between the GWAS data for selection and estimating  $\gamma_j$ . In addition, the confidence intervals do get narrower with GRAPPLE for T2D, showing the potential benefit of including weak instruments for less powerful GWAS studies.

Finally, we demonstrate that the three-sample design to avoid selection bias is necessary not only for GRAPPLE, but also for other MR methods. As shown in Fig S1a, the two-sample design where we use the same cohort of the risk factor for selection can result in biased casual effects estimation, and the biases appear for most MR methods even when only the strongly associated SNPs are selected.

### 2.2.2 Level of pleiotropy in SNPs with heterogeneous strengths

Next, we examine whether or not the weak instruments are more vulnerable to pleiotropy, which can be a concern for including the weak SNPs. We compare four risk factor and disease pairs that cover eight different complex traits, including the effect of BMI on T2D, low-density cholesterol concentrations (LDL-C) on coronary artery disease (CAD), height on smoking, and systolic blood pressure (SBP) on stroke (Fig 2b).

We test whether independent sets of strongly and weakly associated SNPs can provide consistent estimates of the causal effects of the risk factors. SNPs passing the p-value threshold  $10^{-2}$  in the cohort for selection are divided into three groups after LD clumping: “strong” ( $p_j \leq 10^{-8}$ ), “moderate” ( $10^{-8} < p_j \leq 10^{-5}$ ), and “weak” ( $10^{-5} < p_j \leq 10^{-2}$ ). The SNPs across groups are used separately to obtain group-specific estimates of the causal effect  $\beta$ . We observe that for all the four pairs, the estimates  $\hat{\beta}$  are stable across groups (Fig 2b). Though the “weaker” SNPs provide estimates with more uncertainty due to limited power, the estimates are consistent with those from the “strong” group. Other MR methods also show some level of consistency in estimating  $\beta$  across different sets of instruments, but perform worse due to weak instrument bias (Fig S1b). To conclude, in the analysis of these four pairs of traits, we do not see any evidence that weakly associated SNPs provide more biased estimates than strong instruments due to horizontal pleiotropy. In contrast, as the strong SNPs, they may also provide useful information to infer the causal effects of the risk factors. GRAPPLE can expand the ability to evaluate causal effect of risk factors with both strong and weak genetic instruments.

### 2.2.3 Identify direction of causality for known causal relationships

Then, we examine the performance of GRAPPLE in identifying the causal direction with the shape of the profile likelihood. For the causal direction, we focus on the two pairs of traits with known causal relationship: BMI on T2D, and LDL-C on CAD. We switch the roles of the risk factor and

disease to see if the correct direction can be revealed. Specifically, we treat T2D and CAD as the “risk factor”, and BMI and LDL-C as the corresponding “disease” (Fig 2c). For T2D, the cohort for the other gender is used for SNP selection and for CAD, the risk factor cohort used is from [17] and the selection p-values are from [44]. As expected, we see that when the roles of the risk factor and disease are reversed, the robustified profile likelihood shows a main mode at 0, and a weaker mode around  $1/\beta$ .

## 2.2.4 Multiple pleiotropic pathways in the effect of C-reactive protein

Finally, we test for our ability to identify multiple pleiotropic pathways with the analysis of the C-reactive protein (CRP) effect on CAD. C-reactive protein has been found to be strongly associated with the risk of heart disease while many SNPs who are associated with the C-reactive protein also seem to have pleiotropic effect on lipid traits [22]. Previous MR analyses only included SNPs that are near the gene CRP to guarantee a free-of-pleiotropy analysis [14] and found that CRP has no causal effect on CAD, validated also by randomized experiments [28]. However, if the SNP selection near CRP gene is not performed, can GRAPPLE identify the existence of multiple pathways and obtain the correct estimate of the C-reactive protein effect from its associated SNPs across the whole genome?

CRP GWAS data from [40] is used for selection and the data from [20] using a larger cohort is used for getting  $\hat{\gamma}_j$ . The robustified profile likelihood shows a pattern of three modes, indicating the existence of at least three different pathways (Fig 2d). One mode is negative, one is positive and the third is around zero. The negative mode involves a few marker genes including *HNF1A* and *PVRL2*, with a marker trait LDL-C. The positive mode has marker traits pulmonary function and the C-reactive protein, and the few markers genes (*IL6R*, *ARHGAP10*, *BCL7B*, *PABPC4*) are also involved in immune response and lung cancer progression [47, 48]. The mode at 0 has marker genes *CRP* and *LEPR*, and only one marker trait, the C-reactive protein.

We compare across 3 p-value thresholds ( $10^{-8}$ ,  $10^{-5}$ ,  $10^{-3}$ ) and check how the existence of multiple pathways affects causal estimates of the effect of C-reactive protein in MR methods using SNPs across the genome. Including the C-reactive protein as the only risk factor, all bench-marking methods give a negative estimate of the CRP effect, which is possibly driven by the bias from an LDL-C induced pleiotropic pathway (Fig 2e). MR-RAPS is the estimation method used in GRAPPLE only there is only one risk factor, and the three other bench-marking methods give incorrect inference of the CRP effect with a p-value of  $\beta$  below 0.01 for at least one SNP selection threshold (notice that the weak instrument bias is bias towards *zero* as shown in Fig 2a, thus the significance at p-value threshold  $10^{-3}$  for MR-Egger and IVW is not due to weak instrument bias). In contrast, after using two risk factors: the C-reactive protein and LDL-C, where LDL-C is an apparent confounding risk factor from Fig 2d, the estimates of CRP effect can keep insignificant across p-value thresholds. In addition, the estimates  $\hat{\beta}_{CRP}$  themselves are much closer to 0 compared with that without including LDL-C. This analysis illustrates how GRAPPLE can detect pleiotropic pathway, provide information on which confounding risk factors to adjust for, and obtain reliable inference after adjusting for additional risk

323 factors.

324 As a complement to the above real data analysis, we have also conducted a set of simulations  
325 to evaluate GRAPPLE’s performance in detecting multiple pleiotropic pathways. For details, see  
326 Supplementary Note 2 and Fig S2.

### 327 **2.3 A causal landscape from 5 risk factors to 25 common diseases**

328 Finally, we apply GRAPPLE to interrogate the causal effects of 5 risk factors on 25 complex diseases  
329 through a multivariate genome-wide screen. The five risk factors are three plasma lipid traits: LDL-C,  
330 high-density lipoprotein cholesterol (HDL-C), triglycerides (TG), BMI and SBP. The diseases include  
331 heart disease, Type II diabetes, kidney disease, common psychiatric disorders, inflammatory disease  
332 and cancer (Fig 3a). For each pair of the risk factor and disease, we compare across p-value thresholds  
333 from  $10^{-8}$  to  $10^{-2}$ . As a summary of the results, Fig 3a illustrates the average number of modes  
334 detected across the p-value thresholds for SNP selection (for modes at each p-value threshold, see  
335 Figure S2). Besides the number of modes, Fig 3a also shows the p-values for each risk factor when  
336 GRAPPLE is performed with only the single risk factor (see also Fig S3, Materials and Methods).  
337 These p-values are not valid when there are pleiotropic pathways.

338 Fig 3a shows that multi-modality can be detected in many risk factor and disease pairs. Multi-  
339 modality is most easily seen using the stringent p-value threshold  $10^{-8}$  (Fig S3). However, we find  
340 that some modes are contributed by a single SNP thus is more likely an outlier than a pathway. For  
341 instance, the effect of stroke on LDL-C shows two modes when the p-value threshold is  $10^{-8}$  or  $10^{-7}$   
342 (one mode around  $-2.3$  and another mode near  $0.08$ ). However, the negative mode only has one  
343 marker SNP (rs3184504) which has been found strongly associated with hundreds of different traits  
344 according to GWAS Catalog [9] while the other mode has hundreds or marker genes. After removing  
345 the SNP rs3184504, the mode disappears. Such a mode also disappears when we increase the p-value  
346 threshold to include more SNPs as instruments. Thus, the average number of modes serves as a  
347 strength of evidence for the existence of multiple pleiotropic pathways. Some risk factor and disease  
348 pairs show multi-modality without having a significant p-value for  $\beta$ , suggesting that the risk factor  
349 and disease are genetically correlated through multiple pathways but there is no evidence that risk  
350 factor has a causal effect on the disease.

351 We then focus on two diseases: CAD and T2D. For CAD, all five risk factors show very significant  
352 effects, though multi-modality is detected in HDL-C and SBP. First, consider the well-studied, often-  
353 debated relationship between CAD and the lipid traits. In our results for HDL-C, with different  
354 p-value thresholds, three modes in total can show up, two being negative and one positive, indicating  
355 that the pathways from HDL-C to CAD is complicated (Fig 3b). (Fig 3b shows that one negative mode  
356 is contributed by SNPs near genes *LPL* and *BUD13*, which are strongly associated with triglycerides.  
357 Another positive mode is contributed by SNPs near genes *ALDH1A2* and *PSKH1*, which is related  
358 to respiratory diseases [52]. The markers of the other negative mode are mapped to genes including  
359 *LIPG* and *CETP*.

360 Since the effects of the lipid traits are generally complicated, we combine all 5 risk factors and run

361 an MR jointly with GRAPPLE (Fig 3c) with different p-value thresholds. After adjusting for other  
362 risk factors, the two most prominent risk factors for the heart disease are LDL-C and SBP, while the  
363 protective effect of HDL-C stays negligible as well as the risk brought by TG. So these results show  
364 that HDL-C as a single measurement does not seem to have a protective effect on heart disease, while  
365 there are complicated multiple pathways involved. Researchers have suggested analyzing different  
366 subgroups of HDL-C as smaller particles tend to have a stronger protective effect [60].

367 Lipids are involved in a number of biological functions including energy storage, signaling, and  
368 acting as structural components of cell membranes and have been reported to be associated with  
369 various diseases [54, 24, 56, 27, 34, 1]. Besides CAD, another disease that most likely involves the lipid  
370 traits is the Type II diabetes (Fig 3a). T2D is associated with dyslipidemia (i.e., higher concentrations  
371 of TG and LDL-C, and lower concentrations of HDL-C), though the causal relationship is still unclear  
372 [23]. In the mean time, evidence has emerged that LDL-C reduction with statin therapy results in a  
373 modest increase in risk of T2D [54]. For the MR analyzing each risk factor alone, we see potential  
374 protective effects of LDL-C and HDL-C on T2D but also multi-modality patterns. Two modes show  
375 up in the profile likelihood from HDL-C to T2D where one negative mode has a marker gene *LPL*  
376 and a mode near 0 with marker genes *CETP* and *AC012181.1*. Thus we include all 3 lipid traits,  
377 along with *BMI* and run a joint model for these 4 risk factors using GRAPPLE (Fig 3d). Our result  
378 indicates a mild protective effect of HDL-C on T2D, while showing not enough evidence for the effect  
379 of either LDL-C or TG.

### 380 **3 Discussion**

381 We propose a comprehensive framework that utilizes both strong and weakly associated SNPs to un-  
382 derstand the causal relationship between complex traits. GRAPPLE is robust to pervasive pleiotropy  
383 and can identify multiple pleiotropic pathways. The multivariate MR in GRAPPLE can adjust for  
384 known confounding risk factors.

385 GRAPPLE incorporates several improvements over existing MR methods. It gets rid of weak  
386 instrument bias by dealing with measurement errors of the SNP associations on the risk factors with  
387 profile likelihood. Our likelihood is similar to the approach in [12], while allowing pervasive pleiotropy  
388 with the inSIDE assumption. The multi-modality visualization shares similarities with [25], which  
389 estimates the causal effect by the global mode, but we provide a more comprehensive analysis to  
390 identify multiple pleiotropic pathways by the local modes. Our causality direction identification is  
391 related to bidirectional MR where they used the assumption that if we reverse the role of risk factor  
392 and disease, the estimated causal effect is likely to be 0. We use this idea in a more principled way  
393 and can avoid bias when SNPs affecting the disease through the target risk factors are also selected  
394 in the reversed MR. Finally, as the intercept term in MR-Egger is not invariant to the arbitrary  
395 assignment of effect alleles for each SNP, leading to the deficiency of the method, GRAPPLE does  
396 not include any intercept term.

397 GRAPPLE needs a separate GWAS cohort of the exposure for SNP selection, which is necessary

398 for valid inference with weakly associated SNPs. Actually, as shown in Fig S1a, the three-sample  
399 design is needed for other MR methods as well to avoid selection bias. Currently, we find it hard  
400 to obtain multiple good-quality public GWAS summary statistics with non-overlapping cohorts. We  
401 suggest that the stage-specific or study-specific GWAS data before meta-analysis may be released to  
402 the public in the future.

403 In GRAPPLE, we still require using a p-value threshold, though it can be as mild as  $10^{-2}$ ,  
404 instead of requiring no p-value threshold at all. There are two main reasons for this requirement.  
405 One consideration is to increase power, as including too many SNPs with  $\gamma_j = 0$  or extremely small  
406 would instead increase the variance of  $\hat{\beta}$  [59, 58]. Another consideration is that we would not want  
407 unmeasured risk factors that are unassociated (or very weakly associated) with target risk factors  
408 to bring in large pleiotropic effects on SNPs that mainly affect these unmeasured risk factors. The  
409 chance of including these SNPs would be much lower by requiring a mild p-value threshold.

410 To adjust for confounding risk factors, GRAPPLE requires that these factors are either known a  
411 priori, or can be identified from the marker SNPs / genes / traits. However, this step can be hard  
412 to execute in practice. The pleiotropic pathways may not be well tagged, and GRAPPLE may not  
413 have the power to return enough markers. As a future direction, instead of adjusting for unknown  
414 confounding risk factors, we may consider directly adjusting for confounding gene expressions that  
415 can be more easily identified.

416 Finally, when discussing the causal effect of a risk factor, one implicit assumption we use is  
417 consistency, assuming that there is a clear and only one version of intervention that can be done  
418 on the risk factor. However, interventions on risk factors such as BMI are typically vague [15]. For  
419 instance, there can be multiple ways to change weight, such as taking exercise, switching to different  
420 diet or conducting a surgery. It is common sense that these different interventions would have different  
421 effects on diseases, though they may change BMI by the same amount. Similarly, the cholesterol has  
422 abundant functions in our body and involves in multiple biological processes. Intervening different  
423 biological processes to change the concentrations of lipid traits may also have different effect on  
424 diseases. With MR, the interventions are changing risk factors levels with natural mutations, which  
425 may be different from interventions with drugs that has a rapid and strong effect on the risk factors.  
426 We think that our causal inference using GRAPPLE, along with the markers we detect, would provide  
427 abundant information to deepen our understanding of the risk factors. However, one still needs to  
428 be careful when giving causal interpretations of the results. One recommendation in practice is to  
429 triangulate the results from MR with other sources of evidence [37].

## Materials and Methods

### Model details

The structural equations (1) where  $\mathbf{X} = (X_1, X_2, \dots, X_K)$  and  $\boldsymbol{\beta} = (\beta_1, \beta_2, \dots, \beta_K)$  describe how individual level data are generated. To link it with the GWAS summary statistics data, denote

$$\gamma_{jk} = \operatorname{argmin}_{\gamma} \operatorname{Var} [X_k - \gamma Z_j]$$

which is the true marginal association between a SNP  $Z_j$  and risk factor  $X_k$  and

$$\alpha_j = \operatorname{argmin}_{\alpha} \operatorname{Var} [f(\mathbf{U}, \mathbf{Z}, E_Y) - \alpha Z_j]$$

which is the marginal association between  $Z_j$  and the causal effects of unmeasured risk factors on  $Y$ , i.e. the horizontal pleiotropic effect of  $Z_j$  on  $Y$  given  $\mathbf{X}$ . Then we can rewrite the structural equations into the following linear models:

$$X_k = \gamma_{jk} Z_j + [g_k(\mathbf{U}, \mathbf{Z}, E_{X_k}) - \gamma_{jk} Z_j] = \gamma_{jk} Z_j + \epsilon_{jk} \quad (5)$$

$$Y = \mathbf{X}^T \boldsymbol{\beta} + \alpha_j Z_j + [f(\mathbf{U}, \mathbf{Z}, E_Y) - \alpha_j Z_j] = \mathbf{X}^T \boldsymbol{\beta} + \alpha_j Z_j + \tilde{e}_j \quad (6)$$

where  $\operatorname{corr}(Z_j, \epsilon_{jk}) = 0$  for any  $k$  and  $\operatorname{corr}(Z_j, \tilde{e}_j) = 0$  guaranteed by the definitions of  $\gamma_{jk}$  and  $\alpha_j$ . By replacing  $\mathbf{X}$  in (6) with (5), we get

$$Y = (\boldsymbol{\gamma}_j^T \boldsymbol{\beta} + \alpha_j) Z_j + \tilde{e}_j + \sum_k \beta_k \epsilon_{jk} = \Gamma_j Z_j + e_j$$

where  $\Gamma_j = \boldsymbol{\gamma}_j^T \boldsymbol{\beta} + \alpha_j$  and  $e_j = \tilde{e}_j + \sum_k \beta_k \epsilon_{jk}$ . As  $\operatorname{Corr}(Z_j, e_j) = 0$ , we conclude that  $\Gamma_j$  also satisfies that

$$\Gamma_j = \operatorname{argmin}_{\Gamma} \operatorname{Var} [Y - \Gamma Z_j].$$

Thus, parameters  $\Gamma_j$  also represent true marginal associations between SNP  $Z_j$  and the the disease trait. This is how we result in working with Eq (2).

When the disease is a binary trait, the structural equation of  $Y$  changes to

$$\operatorname{logit} [P(Y = 1)] = \mathbf{X}^T \boldsymbol{\beta} + f(\mathbf{U}, \mathbf{Z}, E_Y) \quad (7)$$

With the same argument, we have

$$\operatorname{logit} [P(Y = 1)] = \Gamma_j Z_j + e_j$$

If we further assume that for each genetic instrument  $j$ ,  $Z_j$  is actually independent of  $e_j$  (instead of just being uncorrelated), then the odds ratio that is estimated from the marginal logistic regression will be approximately  $\Gamma_j/c$  with a constant  $c > 1$  determined by the distribution of  $e_j$ . In other



words, for binary disease outcomes, Eq (2) is still approximately correct with the  $\beta$  in (2) being a conservatively biased (by a ratio of  $1/c$ ) version of the  $\beta$  in (7) (for a detailed calculation, see A.1 of [59]).

## GWAS summary statistics from overlapping cohorts

The GWAS estimated effect sizes (log odds ratios for binary traits) of SNP  $j$  are  $\hat{\Gamma}_j$  for the disease and a length  $K$  vector  $\hat{\gamma}_j$  for the risk factors. As shown in [7] and derived in Supplementary Note 3.1, for any risk factor  $k$  we have

$$\text{Corr} \left[ \hat{\Gamma}_j, \hat{\gamma}_{jk} \right] \approx \frac{N_{sk}}{\sqrt{N_{ek}N_o}} \text{Corr} [Y_s, X_{ks}] \quad (8)$$

where  $N_o$  and  $N_{ek}$  are the total sample sizes for the disease and  $k$ th risk factor.  $N_{sk}$  is the number of shared samples. The correlation of  $X_k$  and  $Y$  of any shared sample is  $\text{Corr} [Y_s, X_{ks}]$ . Eq (8) shows that all the SNPs share the same correlation. As a consequence, we assume

$$\begin{pmatrix} \hat{\Gamma}_j \\ \hat{\gamma}_j \end{pmatrix} \sim \mathcal{N} \left( \begin{pmatrix} \Gamma_j \\ \gamma_j \end{pmatrix}, \Sigma_j = \begin{pmatrix} \sigma_{Y_j} & & & \\ & \sigma_{X_{j1}} & & \\ & & \ddots & \\ & & & \sigma_{X_{jK}} \end{pmatrix} \Sigma \begin{pmatrix} \sigma_{Y_j} & & & \\ & \sigma_{X_{j1}} & & \\ & & \ddots & \\ & & & \sigma_{X_{jK}} \end{pmatrix} \right) \quad (9)$$

where  $\Sigma$  is the unknown shared correlation matrix.

## Estimate the shared correlation $\Sigma$

To estimate  $\Sigma$  from summary statistics, we can use Eq (8). We first need to choose SNPs where  $\gamma_{jk} = 0$  for all risk factors  $k$  so that we can estimate the shared correlation  $\text{Corr} \left[ \hat{\Gamma}_j, \hat{\gamma}_{jk} \right]$  using the sample correlation of the chosen SNPs. We choose all SNPs whose selection p-values  $p_{jk} \geq 0.5$  for all  $k$ .

For these selected SNPs, denote the Z-values of  $(\hat{\gamma}_j, \hat{\Gamma}_j)$  for  $j = 1, \dots, T$  as matrix  $Z_{T \times (K+1)}$  where  $T$  is the number of selected SNPs. Then  $\Sigma$  is estimated as the correlation matrix of  $Z_{T \times (K+1)}$ .

## Instruments selection using LD clumping

In GRAPPLE, we need to first select a set of SNPs as genetic instruments to estimate the causal effects  $\beta$ . Here, we only select independent SNPs to simplify the calculation. Besides the independence requirement, we only include SNPs that pass a p-value threshold to reduce the inclusion of false positives that can decrease power. To avoid selection bias, a separate cohort for each risk factor is used where the reported p-values in that cohort are used for instruments selection. Denote the selection p-value for SNP  $j$  and risk factor  $k$  as  $p_{jk}$ , for multiple risk factors and a given selection threshold, we require the Bonferroni combined p-values  $K \min(p_{jk})$  to pass the threshold. After that,

we use LD clumping with PLINK [29] to select independent genetic instruments. The LD  $r^2$  threshold for PLINK is set to 0.001.

## Estimate the effects $\beta$

Here, we perform statistical analysis assuming  $\alpha_j \sim N(0, \tau^2)$  for the pleiotropic effects, while robust to outliers where the pleiotropic effects for a few instruments are large.

Under model (9), Eq (2) and given  $\Sigma$ , the log-likelihood with GWAS summary statistics satisfy:

$$L(\beta, \gamma_1, \dots, \gamma_p, \tau^2) = -\frac{1}{2} \sum_{j=1}^p \left[ \begin{pmatrix} \hat{\Gamma}_j - \gamma_j^T \beta \\ \hat{\gamma}_j - \gamma_j \end{pmatrix}^T (\Sigma_j + \tau^2 ee^T)^{-1} \begin{pmatrix} \hat{\Gamma}_j - \gamma_j^T \beta \\ \hat{\gamma}_j - \gamma_j \end{pmatrix} + \log |\Sigma_j + \tau^2 ee^T| \right]$$

up to some additive constant. Here,  $e = (1, 0, \dots, 0)$ .

Define for each SNP  $j$  the statistics

$$t_j(\beta, \tau^2) = \frac{\hat{\Gamma}_j - \hat{\gamma}_j^T \beta}{\sqrt{\sigma_{Y_j}^2 + \beta^T \Sigma_{X_j} \beta - 2\beta^T \Sigma_{X_j Y_j} + \tau^2}} \quad (10)$$

where  $\Sigma_{X_j}$  is the variance of  $\hat{\gamma}_j$  and  $\Sigma_{X_j Y_j}$  is the covariance between  $\hat{\gamma}_j$  and  $\hat{\Gamma}_j$  in  $\Sigma_j$ . Then the profile log-likelihood that profile out parameters  $(\gamma_1, \dots, \gamma_p)$  results in

$$L(\beta, \tau^2) = \max_{(\gamma_1, \dots, \gamma_p)} L(\beta, \gamma_1, \dots, \gamma_p, \tau^2) = -\frac{1}{2} \sum_{j=1}^p [t_j(\beta, \tau^2)^2 + \log |\Sigma_j + \tau^2 ee^T|]$$

As discussed in [59], maximizing  $L(\beta, \tau^2)$  would not give consistent estimate of  $\tau^2$ . Because of this and the goal of making  $\hat{\beta}$  robust to outlier SNPs with large pleiotropic effects, our optimization function is the adjusted robustified profile likelihood defined as

$$l(\beta, \tau^2) = -\sum_j l_j(\beta, \tau^2) = -\sum_j \rho(t_j(\beta, \tau^2)) \quad (11)$$

where  $\rho(\cdot)$  is some robust loss function. By default, GRAPPLE uses the Tukey's Biweight loss function:

$$\rho(r) = \begin{cases} \frac{c^2}{6} [1 - (1 - (r/c)^2)^3] & \text{if } |r| \leq c \\ c^2/6 & \text{otherwise} \end{cases}$$

where  $c$  is set to its common default value 4.6851. We maximize (11) with respect to  $\beta$  as well as solving the following estimating equation for the heterogeneity  $\tau^2$  which is

$$\varphi_2(\beta, \tau^2) = l(\beta, \tau^2) - p\eta = 0 \quad (12)$$

480 where  $\eta = \mathbb{E}[\rho(Z)]$  with  $Z \sim \mathcal{N}(0, 1)$ . The estimating equation satisfies  $\mathbb{E}[\varphi_2(\boldsymbol{\beta}, \tau^2)] = 0$  at the true  
481 values of  $\boldsymbol{\beta}$  and  $\tau^2$ , thus can result in consistent estimate of  $\tau^2$ . For the details of estimating  $\boldsymbol{\beta}$  and  
482  $\tau^2$  as well building confidence intervals for them, see Supplementary Note 3.2.

## 483 Identify pleiotropic pathways via the multi-modality diagnosis

484 We use the mode detection of the robustified profile likelihood (11) to detect multiple pleiotropic  
485 pathways. To increase sensitivity, we set  $\tau^2 = 0$  and reduce the tuning parameter in the Tukey's  
486 Biweight loss function to  $c = 3$ . Here we present a detailed argument on why mode detection can  
487 identify pleiotropic pathways.

If there is a confounding Genetic Pathway 2  $\tilde{X}$ , as shown in Figure 1a, that are missed, then we have the structural equation

$$Y = \beta X + \kappa \tilde{X} + f(U, Z_1, \dots, Z_p, E_Y)$$

488 and also the linear model

$$X = \delta \tilde{X} + \epsilon, \quad \text{Corr}(Z_j, \epsilon) = 0 \quad (13)$$

for a SNP  $j$  that only associate with Genetic Pathway 2 and uncorrelate with  $X$  conditional on  $\tilde{X}$ . Similar to (5), we have

$$X = \gamma_j Z_j + \epsilon_j, \quad \tilde{X} = \tilde{\gamma} Z_j + \tilde{\epsilon}_j$$

Plug in (13), we have

$$\gamma_j = \delta \tilde{\gamma}_j$$

$$\Gamma_j = \beta \gamma_j + \kappa \tilde{\gamma}_j + \alpha_j = (\beta + \kappa/\delta) \gamma_j + \alpha_j$$

489 Thus, if there are enough SNPs like SNP  $j$ , they would contribute to another mode of (4) at  $\beta + \kappa/\delta$ .

490 The same argument works for identification of the causal direction. Say there is another  $\tilde{X}$  that  
491 affects  $Y$  but is uncorrelated with the risk factor  $X$  ( $\delta = 0$ ). The existence of such  $\tilde{X}$  is common,  
492 unless  $X$  is the only heritable risk factor of  $Y$ . SNPs strongly associated with  $\tilde{X}$  would not likely be  
493 selected when  $X$  is the exposure while would appear when the roles of  $X$  and  $Y$  are switched. These  
494 SNPs can be used to identify the causal direction, as as in the reverse MR, they contribute to a mode  
495 at 0, while the SNPs that affect  $Y$  through  $X$  will contribute to a mode at  $1/\beta$ .

## 496 Select marker SNPs and genes for each mode

497 GRAPPLE uses LD clumping with a stringent  $r^2$  ( $= 0.001$ ) threshold to guarantee independence  
498 among the genetic instruments. However, marker SNPs are not restricted to these independent  
499 instruments in order to get more biological meaningful markers. Marker SNPs are selected from a  
500 SNP set  $\mathcal{G}$  where the SNPs are selected using LD clumping with  $r^2$  threshold 0.05.

501 Assume that there are  $M$  modes detected at positions  $\beta_1, \beta_2, \dots, \beta_M$ . Define the residual of SNP

502  $j$  ( $j \in \mathcal{G}$ ) for mode  $m$  as

$$r_{jm} = t_j(\beta_m, 0)$$

503 where  $t_j(\cdot, \cdot)$  is defined in Eq (10). SNP  $j$  is selected as a marker for mode  $m$  if  $|r_{jm'}| > t_1$  for any  
504  $m' \neq m$  and  $|r_{jm}| \leq t_0$ . By default,  $t_1$  is set to 2 and  $t_0$  is set to 1 which gives reasonable results in  
505 practice. When the marker SNPs are selected, GRAPPLE further map the SNPs to ENCODE genes  
506 where the marker SNPs locate and search for the traits that these SNPs are strongly associated  
507 with in GWA studies by querying HaploReg v4.1 [53] using the R package *HaploR*. The ratios  $\hat{\Gamma}_j/\hat{\gamma}_j$   
508 of the marker SNPs are also returned for reference (shown as the vertical bars in Fig 3b).

## 509 Compute replicability p-values across SNP selection thresholds

510 Each p-value shown in Fig 3a summarizes a vector of p-values across 7 different selection p-value  
511 thresholds ranging from  $10^{-8}$  to  $10^{-2}$  for each risk factor and disease pair. It reflects how consistent  
512 the significance is across SNP selection thresholds. Specifically, it is the partial conjunction p-value  
513 [2] for rejecting the null that  $\beta$  is non-zero for at most 2 of the selection thresholds. For a risk factor  
514 and disease pair  $k$ , let the p-values computed by using SNPs selected with the 7 thresholds  $p_{ks}$  where  
515  $s = 1, 2, \dots, 7$ . Then rank them as  $p_{k(1)} \leq p_{k(2)} \leq \dots \leq p_{k(7)}$ , the partial conjunction p-value for the  
516 pair  $k$  is computed as  $5p_{k(3)}$ .

## 517 Code Availability

518 The R package GRAPPLE can be installed from Github at <https://github.com/jingshuw/GRAPPLE>.

## 519 Data Availability

520 All GWAS summary statistics that are used in the analyses of the manuscript are downloaded from  
521 public resources, where most of them are downloaded from the GWAS Catalog [9], and the websites  
522 of GWAS consortium GIANT, DIAGRAM, PGC, GLGC, and UKBiobank. A complete list of the  
523 datasets used in each analysis and where they are from is provided in Supplementary Tables 1 and  
524 2 and Supplementary Note 2. Intermediate results for screening of 5 risk factors on 25 diseases are  
525 available at <https://www.dropbox.com/sh/myh8xgxne8fo17v/AABWJf781VrCGnqNFMLtnqIea?dl=0>.

## 526 Author Contribution

527 J.W. and Q.Z. conceptualize the study and formulate the model, with discussions with D.S. and N.Z..  
528 J.W. developed the method and algorithm, and performed data analysis. J.B. and G.D.S. helped  
529 with designing the validation experiments. G.H. provided data for the GWAS summary statistics of  
530 C-reactive protein and LD clumping. J.W., Q.Z. and N.Z. wrote the paper.

## References

- 531
- 532 [1] A. P. Agouridis, M. Elisaf, and H. J. Milionis. An overview of lipid abnormalities in patients with  
533 inflammatory bowel disease. *Annals of Gastroenterology: Quarterly Publication of the Hellenic*  
534 *Society of Gastroenterology*, 24(3):181, 2011.
- 535 [2] Y. Benjamini and R. Heller. Screening for partial conjunction hypotheses. *Biometrics*,  
536 64(4):1215–1222, 2008.
- 537 [3] C. Berzuini, H. Guo, S. Burgess, and L. Bernardinelli. A bayesian approach to mendelian  
538 randomization with multiple pleiotropic variants. *Biostatistics*, 21(1):86–101, 2020.
- 539 [4] J. Bowden, G. Davey Smith, and S. Burgess. Mendelian randomization with invalid instru-  
540 ments: effect estimation and bias detection through egger regression. *International journal of*  
541 *epidemiology*, 44(2):512–525, 2015.
- 542 [5] J. Bowden, G. Davey Smith, P. C. Haycock, and S. Burgess. Consistent estimation in mendelian  
543 randomization with some invalid instruments using a weighted median estimator. *Genetic epi-*  
544 *demology*, 40(4):304–314, 2016.
- 545 [6] E. A. Boyle, Y. I. Li, and J. K. Pritchard. An expanded view of complex traits: from polygenic  
546 to omnigenic. *Cell*, 169(7):1177–1186, 2017.
- 547 [7] B. Bulik-Sullivan, H. K. Finucane, V. Anttila, A. Gusev, F. R. Day, P.-R. Loh, L. Duncan, J. R.  
548 Perry, N. Patterson, E. B. Robinson, et al. An atlas of genetic correlations across human diseases  
549 and traits. *Nature genetics*, 47(11):1236, 2015.
- 550 [8] B. K. Bulik-Sullivan, P.-R. Loh, H. K. Finucane, S. Ripke, J. Yang, N. Patterson, M. J. Daly,  
551 A. L. Price, B. M. Neale, Schizophrenia Working Group of the Psychiatric Genomics Consortium,  
552 et al. Ld score regression distinguishes confounding from polygenicity in genome-wide association  
553 studies. *Nature genetics*, 47(3):291, 2015.
- 554 [9] A. Buniello, J. A. L. MacArthur, M. Cerezo, L. W. Harris, J. Hayhurst, C. Malangone, A. McMa-  
555 hon, J. Morales, E. Mountjoy, E. Sollis, et al. The nhgri-ebi gwas catalog of published genome-  
556 wide association studies, targeted arrays and summary statistics 2019. *Nucleic acids research*,  
557 47(D1):D1005–D1012, 2019.
- 558 [10] S. Burgess, A. Butterworth, and S. G. Thompson. Mendelian randomization analysis with  
559 multiple genetic variants using summarized data. *Genetic epidemiology*, 37(7):658–665, 2013.
- 560 [11] S. Burgess, C. N. Foley, E. Allara, J. R. Staley, and J. M. Howson. A robust and efficient  
561 method for mendelian randomization with hundreds of genetic variants. *Nature Communications*,  
562 11(1):1–11, 2020.

- 563 [12] S. Burgess and S. G. Thompson. Multivariable mendelian randomization: the use of pleiotropic  
564 genetic variants to estimate causal effects. *American journal of epidemiology*, 181(4):251–260,  
565 2015.
- 566 [13] S. Burgess, S. G. Thompson, and C. C. G. Collaboration. Avoiding bias from weak instruments  
567 in mendelian randomization studies. *International journal of epidemiology*, 40(3):755–764, 2011.
- 568 [14] C Reactive Protein Coronary Heart Disease Genetics Collaboration et al. Association between  
569 C reactive protein and coronary heart disease: Mendelian randomization analysis based on  
570 individual participant data. *Bmj*, 342:d548, 2011.
- 571 [15] S. R. Cole and C. E. Frangakis. The consistency statement in causal inference: a definition or  
572 an assumption? *Epidemiology*, 20(1):3–5, 2009.
- 573 [16] I. S. Consortium. Common polygenic variation contributes to risk of schizophrenia that overlaps  
574 with bipolar disorder. *Nature*, 460(7256):748, 2009.
- 575 [17] Coronary Artery Disease (C4D) Genetics Consortium et al. A genome-wide association study in  
576 europeans and south asians identifies five new loci for coronary artery disease. *Nature genetics*,  
577 43(4):339, 2011.
- 578 [18] G. Davey Smith and S. Ebrahim. ‘Mendelian randomization’: can genetic epidemiology con-  
579 tribute to understanding environmental determinants of disease? *International journal of epi-  
580 demiology*, 32(1):1–22, 2003.
- 581 [19] G. Davey Smith and G. Hemani. Mendelian randomization: genetic anchors for causal inference  
582 in epidemiological studies. *Human molecular genetics*, 23(R1):R89–R98, 2014.
- 583 [20] A. Dehghan, J. Dupuis, M. Barbalic, J. C. Bis, G. Eiriksdottir, C. Lu, N. Pellikka, H. Wallaschof-  
584 ski, J. Kettunen, P. Henneman, et al. Meta-analysis of genome-wide association studies in 80  
585 000 subjects identifies multiple loci for c-reactive protein levelsclinical perspective. *Circulation*,  
586 123(7):731–738, 2011.
- 587 [21] S. Ebrahim and G. D. Smith. Mendelian randomization: can genetic epidemiology help redress  
588 the failures of observational epidemiology? *Human genetics*, 123(1):15–33, 2008.
- 589 [22] P. Elliott, J. C. Chambers, W. Zhang, R. Clarke, J. C. Hopewell, J. F. Peden, J. Erdmann,  
590 P. Braund, J. C. Engert, D. Bennett, et al. Genetic loci associated with c-reactive protein levels  
591 and risk of coronary heart disease. *Jama*, 302(1):37–48, 2009.
- 592 [23] T. Fall, W. Xie, W. Poon, H. Yaghootkar, R. Mägi, J. W. Knowles, V. Lyssenko, M. Weedon,  
593 T. M. Frayling, E. Ingelsson, et al. Using genetic variants to assess the relationship between  
594 circulating lipids and type 2 diabetes. *Diabetes*, page db141710, 2015.



- 595 [24] A. C. R. Fonseca, R. Resende, C. R. Oliveira, and C. M. Pereira. Cholesterol and statins in  
596 alzheimer’s disease: current controversies. *Experimental neurology*, 223(2):282–293, 2010.
- 597 [25] F. P. Hartwig, G. Davey Smith, and J. Bowden. Robust inference in summary data mendelian  
598 randomization via the zero modal pleiotropy assumption. *International journal of epidemiology*,  
599 46(6):1985–1998, 2017.
- 600 [26] G. Hemani, K. Tilling, and G. D. Smith. Orienting the causal relationship between imprecisely  
601 measured traits using gwas summary data. *PLoS genetics*, 13(11):e1007081, 2017.
- 602 [27] J. R. Hibbeln and N. Salem Jr. Dietary polyunsaturated fatty acids and depression: when  
603 cholesterol does not satisfy. *The American journal of clinical nutrition*, 62(1):1–9, 1995.
- 604 [28] M. V. Holmes, M. Ala-Korpela, and G. D. Smith. Mendelian randomization in cardiometabolic  
605 disease: challenges in evaluating causality. *Nature Reviews Cardiology*, 14(10):577, 2017.
- 606 [29] International Schizophrenia Consortium, S. M. Purcell, N. R. Wray, J. L. Stone, P. M. Visscher,  
607 M. C. O’Donovan, P. F. Sullivan, P. Sklar, et al. Common polygenic variation contributes to  
608 risk of schizophrenia and bipolar disorder. *Nature*, 460(7256):748–752, 2009.
- 609 [30] A. E. Justice, T. W. Winkler, M. F. Feitosa, M. Graff, V. A. Fisher, K. Young, L. Barata,  
610 X. Deng, J. Czajkowski, D. Hadley, et al. Genome-wide meta-analysis of 241,258 adults ac-  
611 counting for smoking behaviour identifies novel loci for obesity traits. *Nature communications*,  
612 8:14977, 2017.
- 613 [31] R. M. Krauss. Lipids and lipoproteins in patients with type 2 diabetes. *Diabetes care*, 27(6):1496–  
614 1504, 2004.
- 615 [32] P.-R. Loh, G. Bhatia, A. Gusev, H. K. Finucane, B. K. Bulik-Sullivan, S. J. Pollack, T. R.  
616 de Candia, S. H. Lee, N. R. Wray, K. S. Kendler, M. C. O’Donovan, B. M. Neale, N. Pat-  
617 terson, A. L. Price, and S. W. G. o. t. P. G. Consortium. Contrasting genetic architectures  
618 of schizophrenia and other complex diseases using fast variance-components analysis. *Nature*  
619 *Genetics*, 47(12):1385–1392, 2015.
- 620 [33] L. A. Lotta, S. J. Sharp, S. Burgess, J. R. Perry, I. D. Stewart, S. M. Willems, J. Luan, E. Ar-  
621 danaz, L. Arriola, B. Balkau, et al. Association between low-density lipoprotein cholesterol-  
622 lowering genetic variants and risk of type 2 diabetes: a meta-analysis. *Jama*, 316(13):1383–1391,  
623 2016.
- 624 [34] M. Maes, R. Smith, A. Christophe, E. Vandoolaeghe, A. V. Gastel, H. Neels, P. Demedts,  
625 A. Wauters, and H. Meltzer. Lower serum high-density lipoprotein cholesterol (hdl-c) in major  
626 depression and in depressed men with serious suicidal attempts: relationship with immune-  
627 inflammatory markers. *Acta Psychiatrica Scandinavica*, 95(3):212–221, 1997.

- 628 [35] A. P. Morris, B. F. Voight, T. M. Teslovich, T. Ferreira, A. V. Segre, V. Steinthorsdottir, R. J.  
629 Strawbridge, H. Khan, H. Grallert, A. Mahajan, et al. Large-scale association analysis provides  
630 insights into the genetic architecture and pathophysiology of type 2 diabetes. *Nature genetics*,  
631 44(9):981, 2012.
- 632 [36] J. Morrison, N. Knoblauch, J. H. Marcus, M. Stephens, and X. He. Mendelian randomiza-  
633 tion accounting for correlated and uncorrelated pleiotropic effects using genome-wide summary  
634 statistics. *Nature Genetics*, pages 1–7, 2020.
- 635 [37] M. R. Munafò and G. D. Smith. Robust research needs many lines of evidence, 2018.
- 636 [38] L. J. O’Connor, A. P. Schoech, F. Hormozdiari, S. Gazal, N. Patterson, and A. L. Price. Extreme  
637 polygenicity of complex traits is explained by negative selection. *The American Journal of*  
638 *Human Genetics*, 105(3):456–476, 2019.
- 639 [39] L. J. O’Connor and A. L. Price. Distinguishing genetic correlation from causation across 52  
640 diseases and complex traits. *Nature genetics*, 50(12):1728–1734, 2018.
- 641 [40] B. P. Prins, K. B. Kuchenbaecker, Y. Bao, M. Smart, D. Zabaneh, G. Fatemifar, J. Luan, N. J.  
642 Wareham, R. A. Scott, J. R. Perry, et al. Genome-wide analysis of health-related biomarkers in  
643 the uk household longitudinal study reveals novel associations. *Scientific reports*, 7(1):1–9, 2017.
- 644 [41] S. Purcell, B. Neale, K. Todd-Brown, L. Thomas, M. A. Ferreira, D. Bender, J. Maller, P. Sklar,  
645 P. I. De Bakker, M. J. Daly, et al. Plink: a tool set for whole-genome association and population-  
646 based linkage analyses. *The American journal of human genetics*, 81(3):559–575, 2007.
- 647 [42] G. Qi and N. Chatterjee. Mendelian randomization analysis using mixture models for robust  
648 and efficient estimation of causal effects. *Nature Communications*, 10(1):1–10, 2019.
- 649 [43] E. Sanderson, W. Spiller, and J. Bowden. Testing and correcting for weak and pleiotropic  
650 instruments in two-sample multivariable mendelian randomisation. *bioRxiv*, 2020.
- 651 [44] H. Schunkert, I. R. König, S. Kathiresan, M. P. Reilly, T. L. Assimes, H. Holm, M. Preuss,  
652 A. F. Stewart, M. Barbalic, C. Gieger, et al. Large-scale association analysis identifies 13 new  
653 susceptibility loci for coronary artery disease. *Nature genetics*, 43(4):333–338, 2011.
- 654 [45] H. Shi, G. Kichaev, and B. Pasaniuc. Contrasting the genetic architecture of 30 complex traits  
655 from summary association data. *The American Journal of Human Genetics*, 99(1):139–153,  
656 2016.
- 657 [46] G. D. Smith, M. V. Holmes, N. M. Davies, and S. Ebrahim. Mendel’s laws, mendelian ran-  
658 domization and causal inference in observational data: substantive and nomenclatural issues.  
659 *European Journal of Epidemiology*, pages 1–13, 2020.

- 660 [47] S. Spencer, S. Köstel Bal, W. Egner, H. Lango Allen, S. I. Raza, C. A. Ma, M. Gürel, Y. Zhang,  
661 G. Sun, R. A. Sabroe, et al. Loss of the interleukin-6 receptor causes immunodeficiency, atopy,  
662 and abnormal inflammatory responses. *Journal of Experimental Medicine*, 216(9):1986–1998,  
663 2019.
- 664 [48] J.-P. Teng, Z.-Y. Yang, Y.-M. Zhu, D. Ni, Z.-J. Zhu, and X.-Q. Li. The roles of arhgap10 in  
665 the proliferation, migration and invasion of lung cancer cells. *Oncology letters*, 14(4):4613–4618,  
666 2017.
- 667 [49] N. J. Timpson, C. M. Greenwood, N. Soranzo, D. J. Lawson, and J. B. Richards. Genetic  
668 architecture: the shape of the genetic contribution to human traits and disease. *Nature Reviews*  
669 *Genetics*, 19(2):110, 2018.
- 670 [50] N. J. Timpson, B. G. Nordestgaard, R. M. Harbord, J. Zacho, T. M. Frayling, A. Tybjærg-  
671 Hansen, and G. D. Smith. C-reactive protein levels and body mass index: elucidating direc-  
672 tion of causation through reciprocal mendelian randomization. *International journal of obesity*,  
673 35(2):300–308, 2011.
- 674 [51] M. Verbanck, C.-y. Chen, B. Neale, and R. Do. Detection of widespread horizontal pleiotropy in  
675 causal relationships inferred from mendelian randomization between complex traits and diseases.  
676 *Nature genetics*, 50(5):693–698, 2018.
- 677 [52] J. Wang, F. Li, H. Wei, Z.-X. Lian, R. Sun, and Z. Tian. Respiratory influenza virus infection  
678 induces intestinal immune injury via microbiota-mediated th17 cell-dependent inflammation.  
679 *Journal of Experimental Medicine*, 211(12):2397–2410, 2014.
- 680 [53] L. D. Ward and M. Kellis. Haploreg: a resource for exploring chromatin states, conservation,  
681 and regulatory motif alterations within sets of genetically linked variants. *Nucleic acids research*,  
682 40(D1):D930–D934, 2012.
- 683 [54] J. White, D. I. Swerdlow, D. Preiss, Z. Fairhurst-Hunter, B. J. Keating, F. W. Asselbergs,  
684 N. Sattar, S. E. Humphries, A. D. Hingorani, and M. V. Holmes. Association of lipid fractions  
685 with risks for coronary artery disease and diabetes. *JAMA cardiology*, 1(6):692–699, 2016.
- 686 [55] N. R. Wray, C. Wijmenga, P. F. Sullivan, J. Yang, and P. M. Visscher. Common disease is more  
687 complex than implied by the core gene omnigenic model. *Cell*, 173(7):1573–1580, 2018.
- 688 [56] R. S. Yadav and N. K. Tiwari. Lipid integration in neurodegeneration: an overview of alzheimer’s  
689 disease. *Molecular neurobiology*, 50(1):168–176, 2014.
- 690 [57] J. Yang, B. Benyamin, B. P. McEvoy, S. Gordon, A. K. Henders, D. R. Nyholt, P. A. Madden,  
691 A. C. Heath, N. G. Martin, G. W. Montgomery, M. E. Goddard, and P. M. Visscher. Common  
692 SNPs explain a large proportion of the heritability for human height. *Nature Genetics*, 42(7):565–  
693 569, 2010.

- 694 [58] Q. Zhao, Y. Chen, J. Wang, and D. S. Small. Powerful three-sample genome-wide design and  
695 robust statistical inference in summary-data Mendelian randomization. *International Journal of*  
696 *Epidemiology*, 48(5):1478–1492, 07 2019.
- 697 [59] Q. Zhao, J. Wang, G. Hemani, J. Bowden, D. S. Small, et al. Statistical inference in two-sample  
698 summary-data mendelian randomization using robust adjusted profile score. *Annals of Statistics*,  
699 48(3):1742–1769, 2020.
- 700 [60] Q. Zhao, J. Wang, Z. Miao, N. Zhang, S. Hennessy, D. S. Small, and D. J. Rader. The role of  
701 lipoprotein subfractions in coronary artery disease: A mendelian randomization study. *bioRxiv*,  
702 page 691089, 2019.

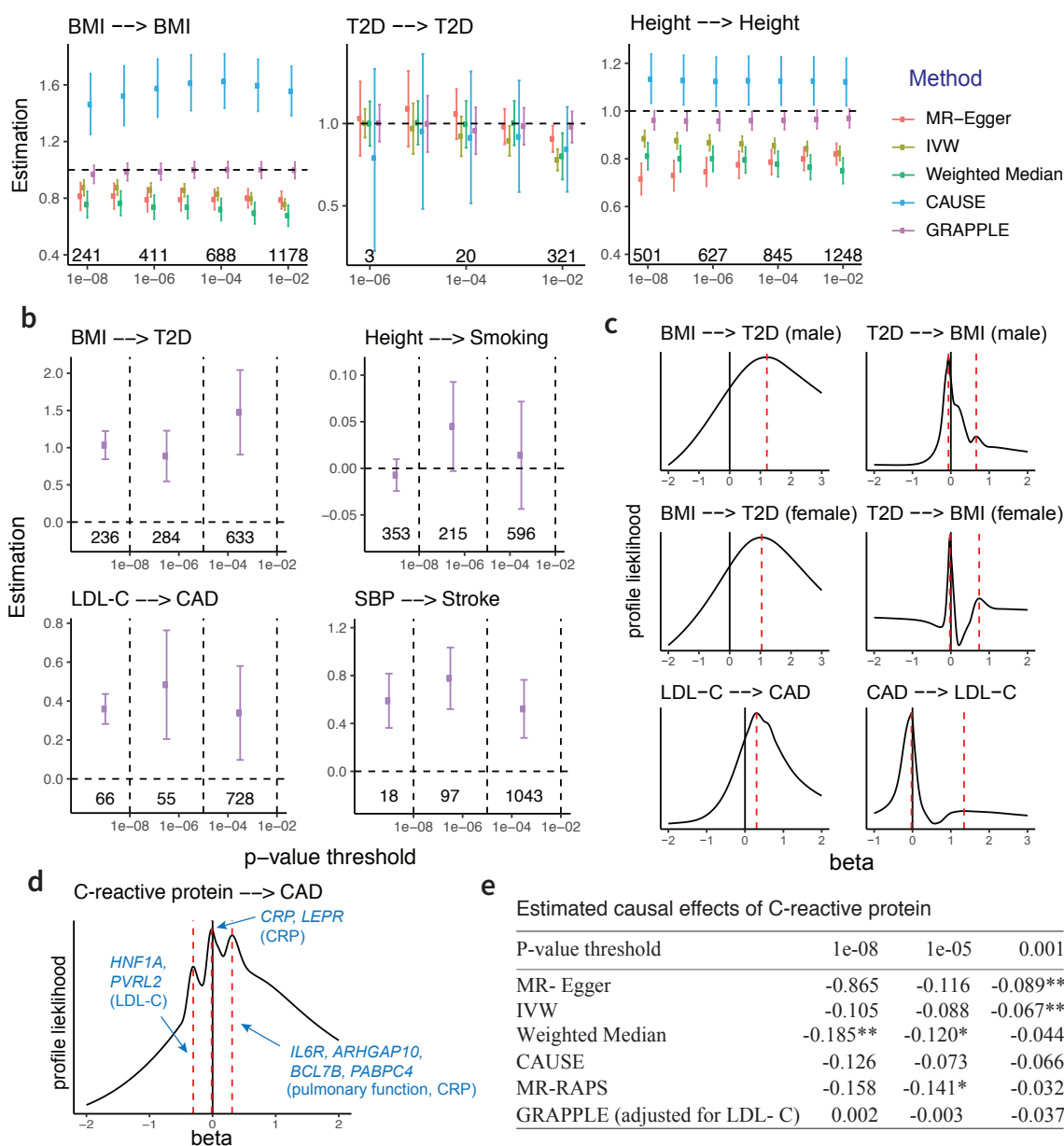


Figure 2: Performance evaluation. **a**, Estimation of  $\beta$  across selection p-value thresholds under no pleiotropy. Error bars show 95% Confidence intervals and the numbers are the number of independent SNPs obtained at each threshold. **b**, Estimation of  $\beta$  across three categories of SNPs. The numbers are the number of SNPs in each category. **c**, Identifying causal directions by multi-modality with MR reversely performed. The selection p-value threshold is kept at  $10^{-4}$ . **d**, three modes detected in the profile likelihood with selection p-value threshold  $10^{-4}$  for CRP on CAD. Marker genes and GWAS traits (in parenthesis) are shown for each mode. **e**, estimation of the CRP effect  $\beta$  at different p-value selection threshold with each method. The numbers are the estimated  $\hat{\beta}$ , with \* indicating p-value below 0.05 and \*\* indicating p-value below 0.01.

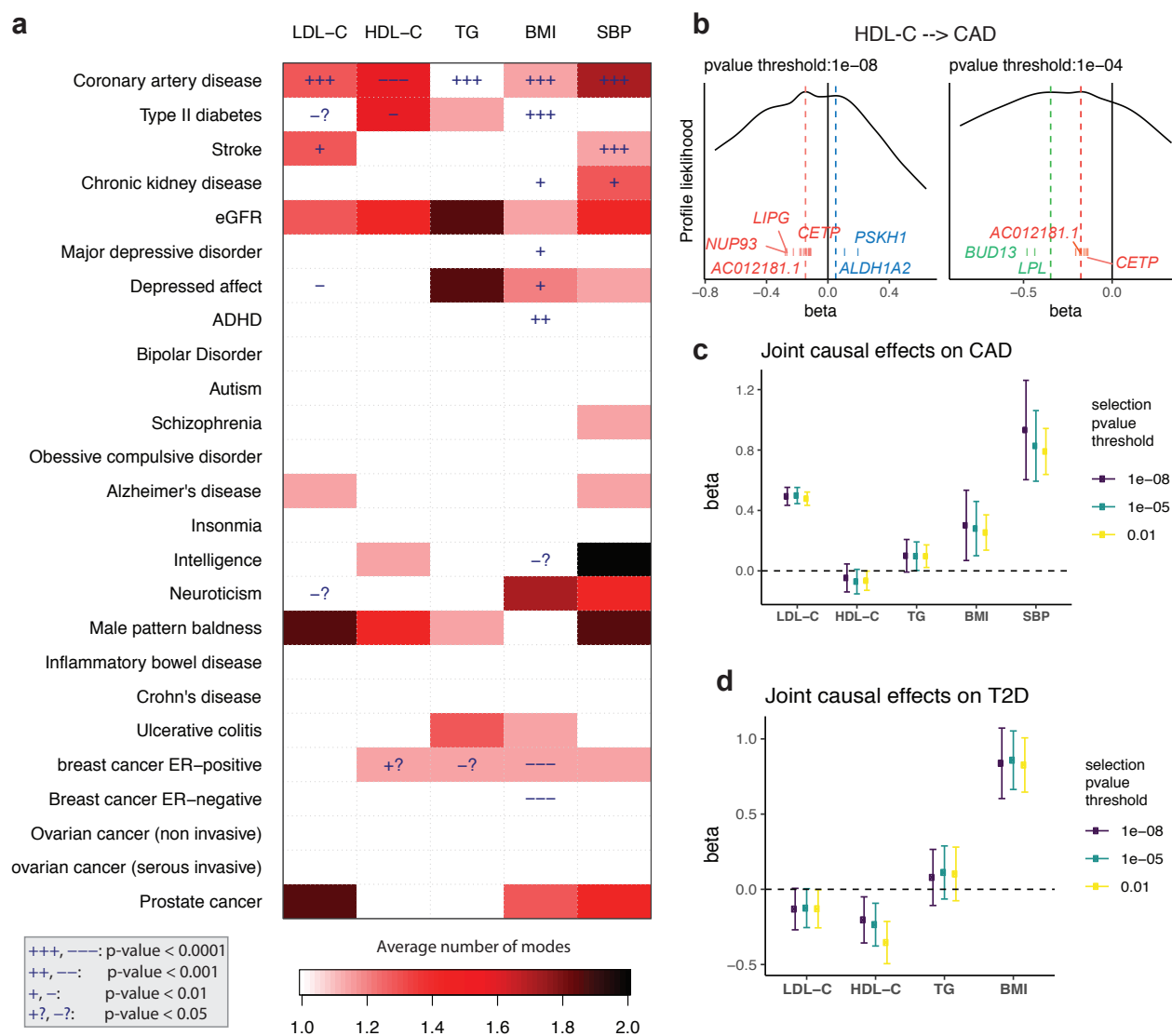


Figure 3: Screening with GRAPPLE. **a**, Landscape of pleiotropic pathways on 25 diseases. The colors show average number of modes across 7 different selection p-value thresholds. The “+” sign shows a positive estimated effect and “-” indicates a negative estimated effect, with the p-value for each cell a combined p-value of replicability across 7 thresholds. These p-values are not multiple-testing adjusted across pairs. **b**, Multi-modality of the profile likelihood for effect of HDL-C on CAD at 2 different selection p-value threshold. Vertical bars are positions of marker SNPs ( $\hat{\Gamma}_j/\hat{\gamma}_j$ ), labeled by their mapped genes (only unique gene names are shown). **c**, Multivariate MR for the effect of 5 risk factors on CAD. **d**, Multivariate MR for the effect of 4 risk factors on CAD. The Error bars are 95% confidence intervals.